2018 26th Mediterranean Conference on Control and Automation (MED)
Zadar, Croatia, June 19-22, 2018

Vector Field based Guidance Law for Intercepting Maneuvering Target

Suwon Lee, Seokwon Lee, Sungjun Ann, Jaeho Lee, and Youdan Kim
Department of Mechanical and Aerospace Engineering
Seoul National University
Seoul, Republic of Korea, 08826
Email: lsw7169@snu.ac.kr

***Abstract*—A vector field based guidance law for intercepting maneuvering target is proposed. The vector field based guidance laws are easy to implement and show high accuracy in a path following problems. To adopt the vector field based guidance law for the missile system, target interception problem is considered as path following problems. After modeling the predicted target trajectory as an implicit function, a vector field is calculated to make missile converge to the predicted target trajectory. The performance of the proposed guidance law is demonstrated by numerical simulations comparing the interception performance with that of proportional navigation guidance laws. The vector field based guidance law shows high interception accuracy (small miss distance) and accomplishes ideal head-on interception.**

I. Introduction

Various guidance laws for the interception of a target have been studied. Proportional navigation (PN) guidance law is one of the most popular methods for missile homing guidance, which was first introduced by Yuan [1]. Owing to its simplicity and guaranteed performance, PN has been studied extensively [2]. The line of sight (LOS) based guidance laws have been extensively studied and designed [3] which include sliding mode guidance and its variations such as nonsingular terminal sliding mode guidance [4] and finite time sliding mode guidance [5] to deal with maneuvering targets and finite time convergence. However, there are some shortcomings. i.e., i) reliance on LOS rate information, ii) lack of full use of predicted target trajectory, and iii) difficulties on analysis.

On the other hand, guidance laws not based on LOS have been also studied, for example, differential geometry based guidance law [6]. Using differential geometry, the target trajectory can be appropriately modeled as geometric curves. Differential geometry based guidance law considers the target's trajectory as geometric curves having certain properties. By utilizing the properties, the differential geometry based guidance law can achieve small miss distance and its performance can be easily analyzed. Despite the benefits, differential geometry based guidance highly depends on the target information, which requires an accurate estimation of the target trajectory.

Vector field based guidance law [7] is one of the guidance laws that one not based on LOS. It was initially developed for solving path following problems, not for target interception problems. Vector field based guidance law in n dimensions was studied by Goncalves et al. [8], and was used in UAV path following guidance such as stand-off target tracking problem [9]. It is easy to implement the vector field based guidance laws regardless of the dynamic model, and accurate path following can be achieved by vector field based guidance laws [10]. Therefore, the vector field based guidance laws can be also adopted for missile engagement problems.

In this paper, the benefits of vector field based guidance law are exploited to achieve ideal head-on interception against high-altitude and a high-speed target whose motion is governed by the gravity. In high altitude, aerodynamic effects are negligible and acceleration control of the missile can be achieved by divert and attitude control systems (DACS) rather than fins using aerodynamic forces. The main advantages of the vector field based guidance with respect to high altitude and high-speed target can be summarized as follows; i) ideal head-on interception with high accuracy can be achieved, ii) the guidance law does not depend on LOS rate information, and iii) asymptotic convergence to the target can be analyzed.

The rest of this paper is organized as follows. In Sec.II, the engagement of missile and target is described and parameters and state variables are defined. In Sec.III, vector field guidance scheme for missile interception is introduced. It is also shown that the vector field is stable in the sense of Lyapunov with respect to the origin. Numerical simulations comparing vector field based guidance law and PN guidance are shown in Sec. IV to demonstrate the performance of proposed guidance law. Section V concludes the results.

II. Problem Formulation

A. Engagement of Missile and Target

Consider an engagement between a target T and a interceptor missile M as shown in Fig.1. The reference lines are parallel to the X-axis of inertial frame coordinate, and the missile and the target flight path angles are defined from the reference lines counterclockwise. Target coordinate is defined by translation from the inertial frame coordinate, and the target position is defined as its origin.

In this paper, the missile and the target are considered as point masses. The speed of the missile V_M is constant, and

978-1-5386-7891-6/18/$31.00 ©2018 IEEE

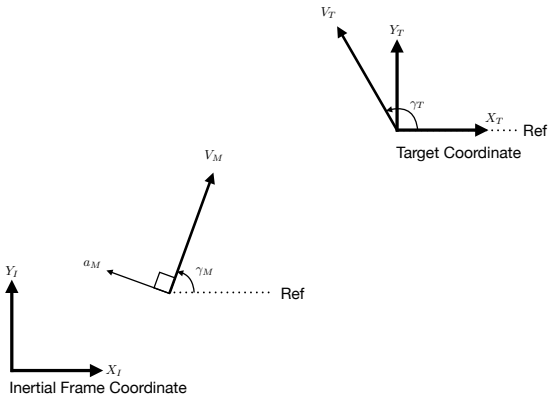

Fig. 1. Simulation results for the network.

the target speed V_T is time-varying because of the accelerating maneuver of the target. The dynamic equations for the interceptor missile can be expressed as

$$\dot{x}_M = V_M \cos\gamma_M \tag{1}$$

$$\dot{y}_M = V_M \sin\gamma_M \tag{2}$$

$$\dot{\gamma}_M = \frac{a_M}{V_M} \tag{3}$$

$$\dot{a}_M = \frac{1}{\tau}(a_{\text{cmd}} - a_M) \tag{4}$$

where γ_M is missile flight path angle, a_M is lateral acceleration given to the missile, and a_{cmd} is lateral acceleration command. The actuator dynamics is modeled by a first order time delay with a time constant τ.

B. Predicted Target Trajectory

The predicted target trajectory should be represented as an implicit equation for the vector field based guidance law. Especially in three dimensional space $[x, y, z] \in \mathbb{R}^3$, the implicit equation $z = f(x, y)$ with implicit function $f(x, y)$ forms two dimensional surface, and $f(x, y) = 0$ forms a curve which is the predicted target trajectory. It is assumed that there always exists partial derivatives of the function $f(x, y)$. Then, the vector field $W(x, y) : \mathbb{R}^2 \to \mathbb{R}^2$ is defined in $x - y$ plane ($z = 0$) using the implicit function $f(x, y)$ and its partial derivatives $\nabla f(x, y)$, which is the gradient vector of $f(x, y)$. The detailed explanation on designing a vector field is described in Sec. III.

Since the vector field based guidance law attracts the missile to the curve expressed in an implicit equation, it is very important to obtain predicted target trajectory accurately. Even though the convergence to the curve is accurately achieved using vector field based guidance law, with an inadequate prediction of the target trajectory, large miss distance may result in.

In this study, the considered engagement of the missile and the target is high altitude environment. In the high altitude environment, the aerodynamic effects on the target such as the aerodynamic forces can be neglected because of low air density. Therefore, the target maneuver in high altitude can be thought as a gravity maneuver, which can be modeled by second-order polynomial or parabola.

Using vector field based guidance, the missile approaches and moves along the predicted target trajectory. If the missile flies against the incoming target trajectory, it is possible to intercept the target with incident angle, the angle between missile velocity and target velocity at the interception, of π, which is an ideal head-on condition.

III. Vector Field based Guidance Law

A. Command Converter Design

A vector field defined in two-dimensional space gives velocity vector at the given (x, y) points. Because it is assumed that the speed of the missile V_M is constant, the flight path angle γ_M is controlled to make a missile follow the velocity vector direction from the vector field $W(x, y) = [\dot{x}_{\text{cmd}}, \dot{y}_{\text{cmd}}]^T$.

$$\gamma_{\text{cmd}} = \arctan\left(\frac{\dot{y}_{\text{cmd}}}{\dot{x}_{\text{cmd}}}\right) \tag{5}$$

Flight path angle error $e \triangleq \gamma_M - \gamma_{\text{cmd}}$ can be made zero by lateral acceleration command $a_{\text{cmd}} = -kV_M e$ with respect to the following error dynamics.

$$\dot{e} = \dot{\gamma} - \dot{\gamma}_{\text{cmd}} = \frac{a_{\text{cmd}}}{V_M} \tag{6}$$

$$= -ke \tag{7}$$

where k is command converter gain.

B. Convergence to the Curve

To compute the vector field $W(x, y)$ in the inertial coordinate, the predicted target trajectory should be obtained as an implicit function $f(x, y) : \mathbb{R}^2 \to \mathbb{R}$ satisfying $f(x, y) = 0$ on the predicted target trajectory. Without loss of generality, one can consider target coordinate whose origin is located at the target point. By applying a proper coordinate transformation, $f(0, 0) = 0$ is satisfied in the target coordinate which makes the curve passes through the origin.

From the assumption, the gradient vector $\nabla f(x, y)$ can be computed everywhere in the target coordinate. The geometric meaning of the gradient vector implies the direction where the value of $f(x, y)$ increases. Therefore, starting from arbitrary initial position $[x_0, y_0]$, it is always possible to reach $[x, y]$ satisfying $f(x, y) = 0$ by moving along gradient direction or negative gradient direction. Therefore, the converging velocity vector can be defined as follows,

$$W_{\text{conv}} \triangleq -\text{sign}(f)\nabla f \tag{8}$$

The converging velocity vector W_{conv} makes the missile converge to $f(x, y) = 0$ or to the target trajectory curve.

C. Traverse along the Curve

Once the missile is attracted to the curve with W_{conv} and converged to the curve, $(f(x,y) = 0)$, the converging velocity vector becomes $W_{\text{conv}} = 0$ on the curve. Then, the missile should traverse along the curve with additional traverse velocity vector W_{trav}. On the curve, the traverse velocity vector is the tangent vector along the curve, i.e.,

$$W_{\text{trav}} \triangleq -\text{sign}(g)\nabla g \tag{9}$$

The orthogonal function $g(x,y) : \mathbb{R}^2 \to \mathbb{R}$ and its gradient vector ∇g can be calculated from the curve function $f(x,y)$ and its gradient vector ∇f. If an implicit function $g(x,y)$ and its gradient vector ∇g satisfy $\nabla f \perp \nabla g$, then $g(x,y)$ is an orthogonal function of $f(x,y)$. Note that the orthogonal function $g(x,y)$ is not unique for a certain $f(x,y)$ because of constant term of the orthogonal function.

In $\mathbb{R}^2$, the orthogonal vector can be easily obtained as

$$\nabla g = \begin{bmatrix} 0 & -1 \\ 1 & 0 \end{bmatrix} \nabla f. \tag{10}$$

The orthogonal function $g(x,y)$ can be calculated by integrating ∇g analytically. By choosing adequate constant of integration, it can be assumed that $g(0,0) = 0$ in the target coordinate.

Figure. 2 describes the vector field and the conceptual diagram. The direction of the vector field is shown with arrows, which converges to the predicted target trajectory and to the target. Note that from Fig. 2 that the vector eld is constructed with respect to the current target position and trajectory, and therefore the missile converges to the impact angle of π for head-on engagement and zero for tail-chase engagement, respectively. In this study, head-on engagement is mainly concerned. In the conceptual diagram, the contours of $f(x,y)$ and $g(x,y)$ are depicted to visualize the direction of the gradient vectors ∇f and ∇g with two orthogonal arrows. The vector field is obtained from the linear combination of the gradient vectors at each point (x,y).

D. Stability Analysis

The vector field $W(x,y)$ can be defined as

$$\begin{aligned} W(x,y) &\triangleq k_f W_{\text{conv}} + k_g W_{\text{trav}} \\ &= -\begin{bmatrix} k_f \nabla f & k_g \nabla g \end{bmatrix} \begin{bmatrix} \text{sign}(f) \\ \text{sign}(g) \end{bmatrix} \\ &= \begin{bmatrix} -k_f \text{sign}(f) \frac{\partial f}{\partial x} - k_g \text{sign}(g) \frac{\partial g}{\partial x} \\ -k_f \text{sign}(f) \frac{\partial f}{\partial y} - k_g \text{sign}(g) \frac{\partial g}{\partial y} \end{bmatrix} \end{aligned} \tag{11}$$

where the weighting factors $k_f, k_g \in [0,1]$, and $k_f + k_g = 1$.

Now, a Lyapunov theorem based stability analysis ensures the following proposition.

Proposition 1: If $f(x,y) = z$ and $g(x,y) = z$ are regular planes in $\mathbb{R}^3$ which have neither self-intersecting points nor sharp points, then a point (x,y) moving along the vector field $W(x,y) = [\dot{x}, \dot{y}]^T$ converges to the origin.

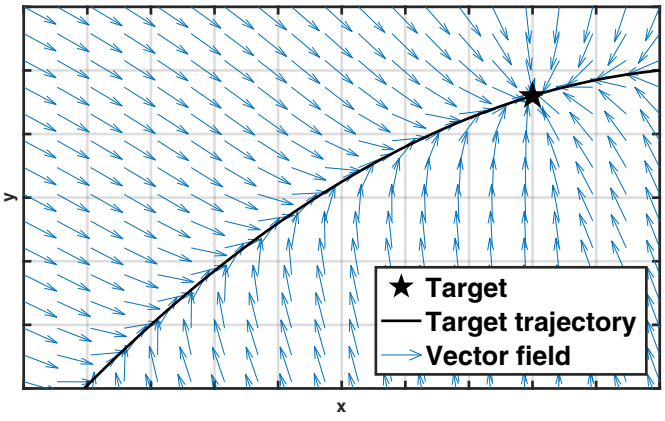

(a)

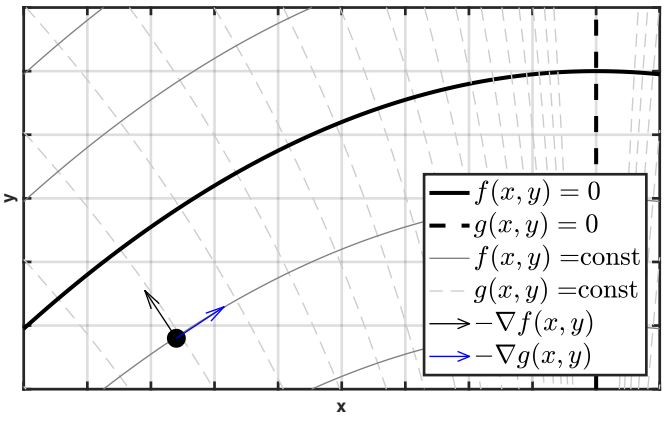

(b)

Fig. 2. (a) Visualization, (b) Conceptual diagram of vector field.

Proof: Let us define a Lyapunov candidate function V as

$$V(x,y) \triangleq \frac{1}{2}\left(k_f f(x,y)^2 + k_g g(x,y)^2\right) \tag{12}$$

Differentiating V with respect to time gives

$$\begin{aligned} \dot{V} &= k_f f \dot{f} + k_g g \dot{g} \\ &= k_f f \nabla f^T [\dot{x}, \dot{y}]^T + k_g g \nabla g^T [\dot{x}, \dot{y}]^T \end{aligned} \tag{13}$$

Substituting $[\dot{x}, \dot{y}]^T = W(x,y)$ into (13), we have

$$\begin{aligned} \dot{V} &= -k_f^2 |f| \nabla f^T \nabla f - k_g^2 |g| \nabla g^T \nabla g \\ &= -k_f^2 |f| \left(\left(\frac{\partial f}{\partial x} \right)^2 + \left(\frac{\partial f}{\partial y} \right)^2 \right) \\ &\quad -k_g^2 |g| \left(\left(\frac{\partial g}{\partial x} \right)^2 + \left(\frac{\partial g}{\partial y} \right)^2 \right) \leq 0 \end{aligned} \tag{14}$$

If $f(x,y) = z$ and $g(x,y) = z$ are regular planes which have neither self-intersecting points nor sharp points, then the equality is satisfied if and only if $(x,y) = (0,0)$. Therefore, a point moving along the vector field $W(x,y)$ converges to the origin by the Lyapunov theorem. ■

TABLE I
SIMULATION CONDITIONS

$P_M(0)$	$[40, 100]$km
$P_T(0)$	$[120, 120]$km
V_M	1000m/s
$V_T(0)$	1500m/s
$\gamma_T(0)$	180deg
a_{limit}	10×9.81m/s

IV. NUMERICAL SIMULATIONS

In this section, the performance of the proposed vector field based guidance law is demonstrated by comparing with PN. Acceleration command using PN guidance can be represented as follows,

$$a_{\text{PN}} = NV_M\dot{\lambda} \tag{15}$$

where N is PN gain and $\lambda \triangleq \gamma_T - \gamma_M$ is line-of-sight angle.

Though PN is designed for the non-maneuvering target, increasing PN gain from 3 to 5 provides improved performance for maneuvering target. The simulation is conducted for a specific initial position and varying missile initial flight path angle to consider head-on interception against faster target than the missile. The simulation conditions are summarized in Table. I.

The predicted target trajectory is modeled as a second-order polynomial because the target maneuvers only by the gravity. The converging function $f(x, y)$ and its orthogonal function $g(x, y)$ is defined in the target coordinate as follows,

$$f(x, y) = y - (ax^2 + bx) \tag{16}$$

$$g(x, y) = -y - \frac{\log(b + 2ax)}{2a} + \frac{\log(b)}{2a} \tag{17}$$

where a and b are scalar coefficients determined by the position and velocity of the target. Note that the origin of the target coordinate is located at the position of the target, and therefore the condition $f(0, 0) = g(0, 0) = 0$ is satisfied and the vector field converges to the target position. The vector field at the missile position P_M in the inertial coordinate can be computed by simply substituting the missile position represented in target coordinate into (16) and (17).

The missile has constant speed and maneuvers with lateral acceleration limit a_{limit}. For numerical simulation, the time constant of the actuator is set as $\tau = 0.15$, and command converter gain k and the vector field gains k_f and k_g are set as 2, 0.7, and 0.3, respectively. For smooth convergence, an alternative vector field is used in simulation: $W_{\text{alt}} = -k_f \cdot \text{tansig}(f \times 10^{-3})\nabla f - k_g \cdot \text{tansig}(g \times 10^{-5})\nabla g$. Tangent sigmoid function is need instead of the sign function to prevent chattering behavior near the curve.

Simulation result of zero, $\pi/4$, and $\pi/2$ initial missile flight path angle cases are shown to understand the maneuvering properties of the missile with vector field based guidance law

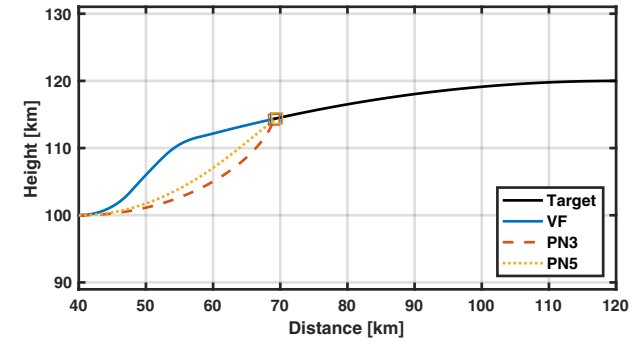

(a)

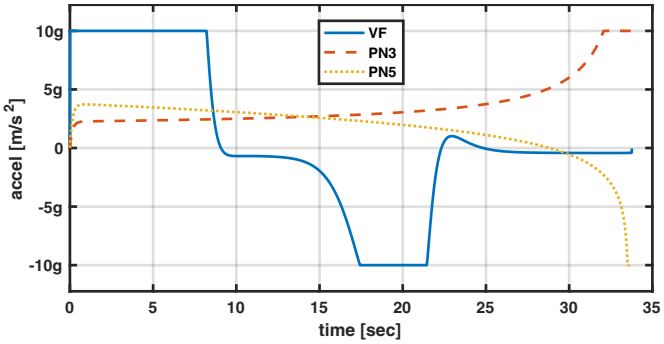

(b)

Fig. 3. Zero initial missile flight path angle case. (a) Trajectories, (b) Lateral acceleration.

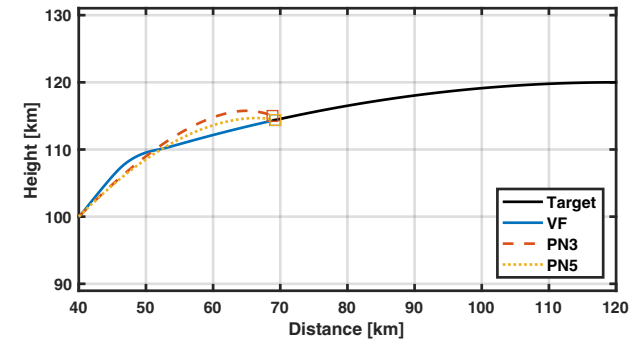

(a)

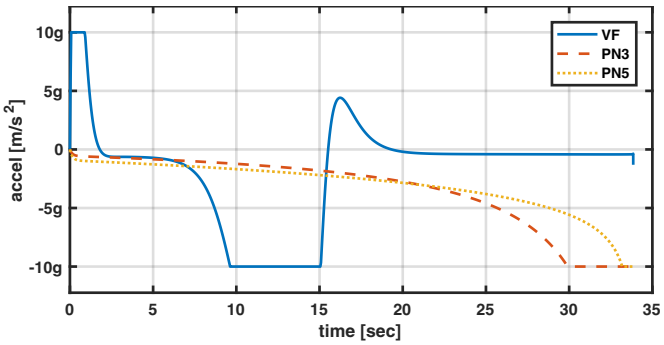

(b)

Fig. 4. $\pi/4$ initial missile flight path angle case. (a) Trajectories, (b) Lateral acceleration.

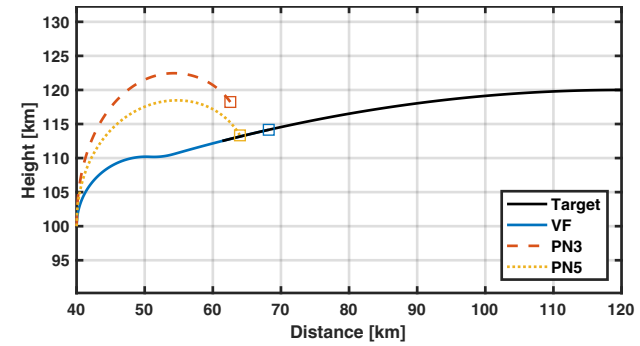

(a)

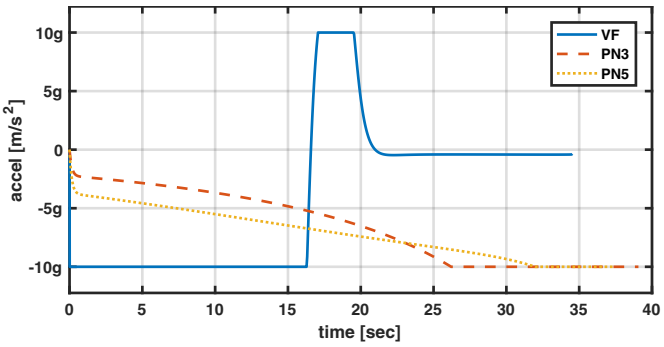

(b)

Fig. 5. $\pi/2$ initial missile flight path angle case. (a) Trajectories, (b) Lateral acceleration.

and to show the performance of vector field based guidance law compared with PNs. The interception and acceleration histories are shown in Figs. 3-5. The missile is first attracted to the predicted target trajectory and traverses along the curve under vector field based guidance law. Ideal head-on interception with the impact angle of π is achieved.

The lateral acceleration history of vector field based guidance law is different from that of PNs. PN3 with $N = 3$ and PN5 with $N = 5$. In general, PNs show an abrupt change of lateral acceleration when the range to the target becomes small because of the rapid change of LOS angle. However, the vector field based guidance law shows large lateral acceleration at the initial and barely uses the lateral acceleration until the missile converges to the curve. Once the missile approaches to the curve, the lateral acceleration is used to line on and traverse along the curve. In summary, the vector field based guidance law consists of two phases of lateral acceleration; i) the first phase to approach curve, and ii) the second phase to line on the curve.

Figure. 6 shows miss distance for various initial missile flight path angles. Note that the vertical axis is in log scale. The vector field based guidance law shows excellent performance compared to PNs in miss distance for every initial missile flight path angle cases.

The relative flight path angle histories are shown in Fig. 7. The relative flight path angle history of vector field based

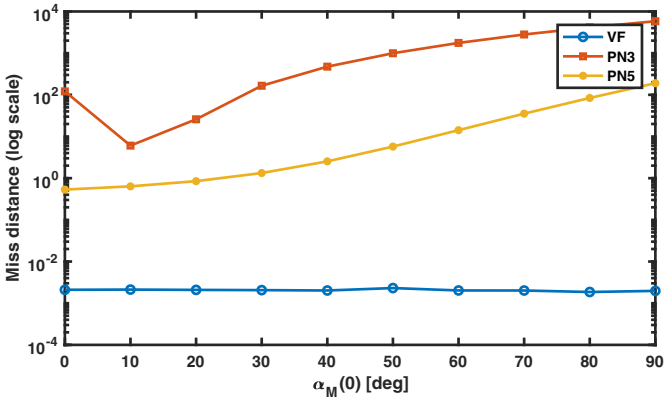

Fig. 6. Miss distances varying initial missile flight path angle. (The vertical axis is in log scale.)

guidance shows similar patterns for the three cases: turn to converging direction, approach the curve, turn to align with the tangent line of the curve, and keep in line with the curve. In contrast, PNs without impact angle constraints would not meet the ideal head-on interception, i.e., impact angle of π.

V. Conclusion

In this paper, vector field based guidance law for missile interception problem was proposed. The vector field based guidance law showed benefits in achieving ideal head-on interception when precise target trajectory information was available. Vector field based guidance law does not rely on line-of-sight information and achieve less miss distance than proportional navigation guidance which relies on line-of-sight information. To demonstrate the effectiveness of the proposed guidance law, numerical simulations with various initial missile flight path angles were carried out. The vector field based guidance law showed appropriate acceleration history compared to the proportional navigation. The miss distance of vector field based guidance law is small with respect to the initial missile flight path angle, while that of the proportional navigation varies affected by the initial value.

The vector field based guidance law can be applied to other path following problems exploiting its simplicity and accuracy. Vector field based guidance law with external disturbances in predicted target trajectory would be further explored to analyze the robustness.

Acknowledgment

This work was conducted at High-Speed Vehicle Research Center of KAIST with the support of the Defense Acquisition Program Administration and the Agency for Defense Development under Contract UD170018CD.

References

[1] L. C. Yuan, Homing and Navigational Courses of Automatic TargetSeeking Devices, J. Appl. Phys., vol. 19, no. 12, pp. 1122-1128, 1948.

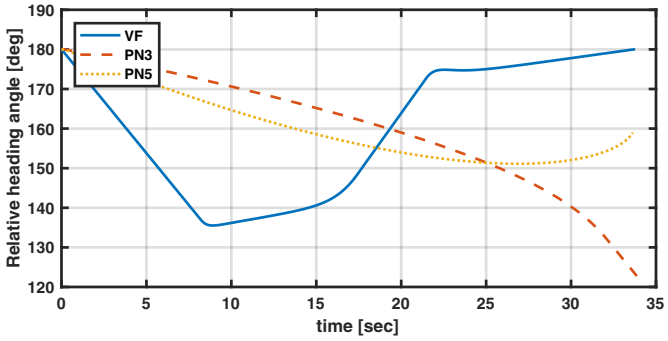

(a)

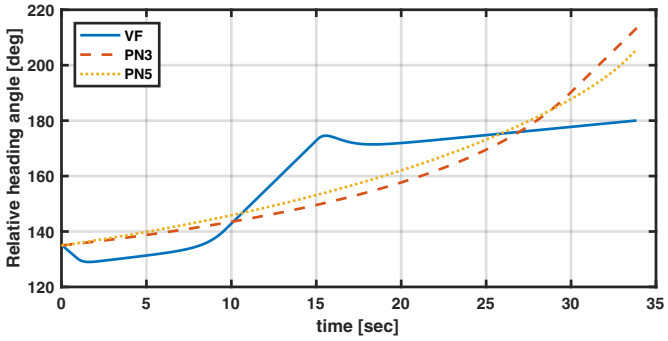

(b)

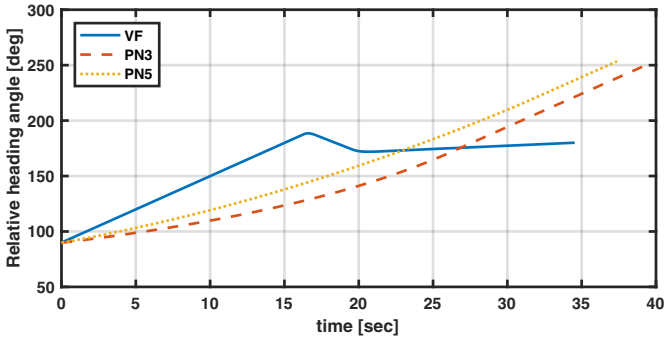

(c)

Fig. 7. Relative flight path angle history. (a) zero initial flight path angle case, (b) $\pi/4$ initial flight path angle case, and (c) π initial flight path angle case.

[2] S. Ghosh, D. Ghose, and S. Raha, Capturability of Augmented Pure Proportional Navigation Guidance Against Time-Varying Target Maneuvers, J. Guid. Control. Dyn., vol. 37, no. 5, pp. 1446–1461, 2014.

[3] B. Zhou and W. Wang, An improved nonsingular fast terminal sliding mode guidance law with impact angle constraints, in 2017 Eighth International Conference on Intelligent Control and Information Processing (ICICIP), 2017, pp. 8-15.

[4] S. R. Kumar, S. Rao, and D. Ghose, Nonsingular Terminal Sliding Mode Guidance with Impact Angle Constraints, J. Guid. Control. Dyn., vol. 37, no. 4, pp. 1114-1130, 2014.

[5] H. S. Shin, A. Tsourdos, and K. B. Li, A New Three-Dimensional Sliding Mode Guidance Law Variation With Finite Time Convergence, IEEE Trans. Aerosp. Electron. Syst., vol. 53, no. 5, pp. 2221-2232, 2017.

[6] O. Ariff, R. Zbikowski, A. Tsourdos, and B. A. White, Differential Geometric Guidance Based on the Involute of the Targets Trajectory, J. Guid. Control. Dyn., vol. 28, no. 5, pp. 990-996, 2005.

[7] D. R. Nelson, D. B. Barber, T. W. McLain, and R. W. Beard, Vector field path following for miniature air vehicles, IEEE Trans. Robot., vol. 23, no. 3, pp. 519-529, 2007.

[8] V. M. Goncalves, L. C. A. Pimenta, C. A. Maia, B. C. O. Dutra, and G. A. S. Pereira, Vector Fields for Robot Navigation Along Time-Varying Curves in n-Dimensions, IEEE Trans. Robot., vol. 26, no. 4, pp. 647-659, 2010.

[9] A. A. Pothen and A. Ratnoo, Curvature-Constrained Lyapunov Vector Field for Standoff Target Tracking, J. Guid. Control. Dyn., vol. 40, no. 10, pp. 2729-2736, 2017.

[10] P. B. Sujit, S. Saripalli, and J. B. Sousa, Unmanned Aerial Vehicle Path Following: A Survey and Analysis of Algorithms for Fixed-Wing Unmanned Aerial Vehicless, IEEE Control Syst., vol. 34, no. 1, pp. 42-59, 2014.